EPJ Web of Conferences **93**, 01007 (2015)
DOI: 10.1051/epjconf/20159301007


# Microscopic analysis of quadrupole-octupole shape evolution

Kosuke Nomura[1,a]

[1] *Grand Accélérateur National d'Ions Lourds, CEA/DSM-CNRS/IN2P3, Bd. Henri Becquerel, B.P.55027, Caen Cedex 5, France*

**Abstract.** We analyze the quadrupole-octupole collective states based on the microscopic energy density functional framework. By mapping the deformation constrained self-consistent axially symmetric mean-field energy surfaces onto the equivalent Hamiltonian of the $sdf$ interacting boson model (IBM), that is, onto the energy expectation value in the boson coherent state, the Hamiltonian parameters are determined. The resulting IBM Hamiltonian is used to calculate excitation spectra and transition rates for the positive- and negative-parity collective states in large sets of nuclei characteristic for octupole deformation and collectivity. Consistently with the empirical trend, the microscopic calculation based on the systematics of $\beta_2 - \beta_3$ energy maps, the resulting low-lying negative-parity bands and transition rates show evidence of a shape transition between stable octupole deformation and octupole vibrations characteristic for $\beta_3$-soft potentials.

## 1 Introduction

The study of equilibrium shapes and shape transitions presents a recurrent theme in nuclear structure physics. Even though most deformed medium-heavy and heavy nuclei exhibit quadrupole, or reflection-symmetric equilibrium shapes, there are regions in the mass table where octupole deformations (reflection-asymmetric, pear-like shapes) occur [1]. Reflection-asymmetric shapes are characterized by the presence of negative-parity bands, and by pronounced electric dipole and octupole transitions. For static octupole deformation, for instance, the lowest positive-parity even-spin states and the negative-parity odd-spin states form an alternating-parity band, with states connected by the enhanced E1 transitions.

Structure phenomena related to reflection-asymmetric nuclear shapes have been extensively investigated in numerous experimental studies (reviewed in [1]). In particular, clear evidence for pronounced octupole deformation in the region $Z \approx 88$ and $N \approx 134$, e.g. in $^{220}$Rn and $^{224}$Ra, has been reported recently [2]. Also some rare-earth nuclei with $Z \approx 56$ and $N \approx 88$ present a good example for octupole collectivity. The renewed interest in studies of reflection asymmetric nuclear shapes using RI beams [2] point to the significance of a timely systematic theoretical analysis of quadrupole-octupole collective states of nuclei in several mass regions of the nuclear chart where octupole shapes are expected to occur.

Meanwhile, a variety of theoretical methods have been applied to studies of reflection asymmetric shapes and the evolution of the corresponding negative-parity collective states. Especially, nuclear energy density functional (EDF) framework enables a complete and accurate description of ground-state properties and collective excitations over the whole nuclide chart [3]. To compute excitation spectra and transition rates, however, the EDF framework has to be extended to take into account the restoration of symmetries broken in the mean-field approximation, and fluctuations in the collective coordinates.

In this work, we perform a microscopic analysis of octupole collective states. We employ a recently developed method [4] for determining the Hamiltonian of the interacting boson model (IBM) [5], starting with a microscopic, EDF-based self-consistent mean-field calculation of deformation energy surfaces. By mapping the deformation constrained self-consistent energy surfaces onto the equivalent Hamiltonian of the IBM, that is, onto the energy expectation value in the boson condensate state, the Hamiltonian parameters are determined. The resulting IBM Hamiltonian is used to compute excitation spectra and transition rates [4]. More recently the method of [4] has been applied to a study of the octupole shape-phase transition in various mass regions [6, 7].

In this contribution, we report the outcome of the recent studies in [6, 7] on the quadrupole-octupole collective states in two characteristic mass regions of octupole deformations, that is, rare-earth (Sm and Ba) and light actinide (Th and Ra) nuclei.

## 2 Mean-field energy surfaces and mapping to boson Hamiltonian

Our analysis starts by performing constrained self-consistent relativistic mean-field calculations for axially symmetric shapes in the ($\beta_2$,$\beta_3$) plane, with constraints on the mass quadrupole $Q_{20}$, and octupole $Q_{30}$ moments. The dimensionless shape variables $\beta_\lambda$ ($\lambda = 2, 3$) are defined in terms of the multipole moments $Q_{\lambda 0}$. The relativistic Hartree-Bogoliubov (RHB) model is used to cal-

[a] e-mail: nomura@ganil.fr

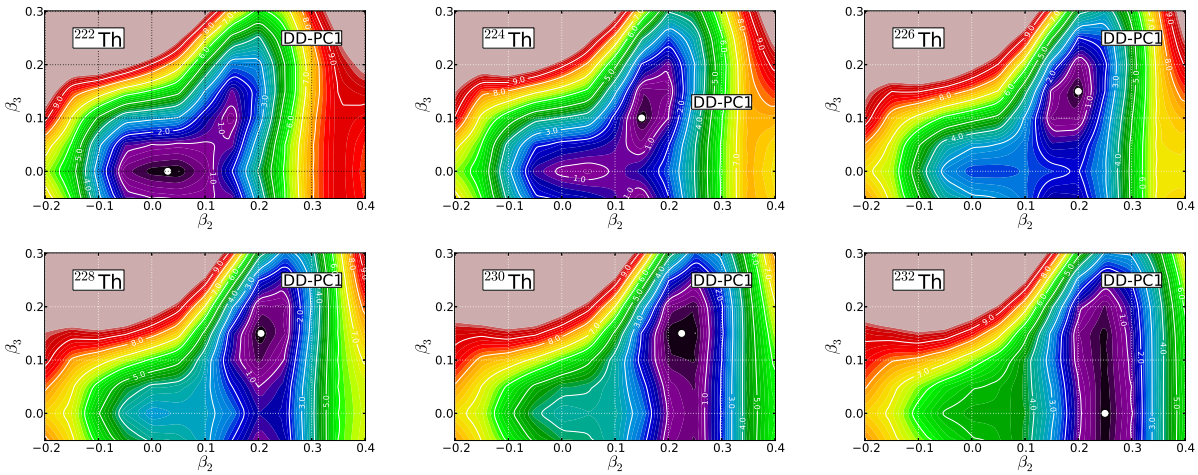


**Figure 1.** (Color online) The DD-PC1 energy surfaces of the isotopes $^{222-232}$Th in the $(\beta_2,\beta_3)$ plane. The color scale varies in steps of 0.2 MeV. The energy difference between neighboring contours is 1 MeV. Open circles denote the absolute energy minima.

culate constrained energy surfaces (cf. [9] for details), the functional in the particle-hole channel is DD-PC1 [10] and pairing correlations are taken into account by employing an interaction that is separable in momentum space, and is completely determined by two parameters adjusted to reproduce the empirical bell-shaped pairing gap in symmetric nuclear matter [8].

As a sample of the RHB calculations, Fig. 1 displays the contour plots of $\beta_2-\beta_3$ deformation energy surfaces for the isotopes $^{222-232}$Th. Already at the mean-field level, the RHB model predicts a very interesting shape evolution. A $\beta_2$-soft energy surface is calculated for $^{222}$Th, with the energy minimum close to $(\beta_2,\beta_3) \approx (0,0)$. The quadrupole deformation becomes more pronounced in $^{224}$Th, and one also notices the development of octupole deformation, with the energy minimum being in the $\beta_3 \neq 0$ region. From $^{224}$Th to $^{226,228}$Th, a rather strongly marked octupole minimum is predicted. The deepest octupole minimum is calculated in $^{226}$Th whereas, starting from $^{228}$Th, the minimum becomes softer in $\beta_3$ direction. Very soft octupole surfaces are obtained for $^{230,232}$Th, the latter being completely flat in $\beta_3$. The energy surfaces for other isotopic chains are found in [7].

To describe reflection-asymmetric deformations and the corresponding negative-parity states, we employ the interacting boson model (IBM) [5], comprising usual positive-parity $s$ ($J^\pi = 0^+$) and $d$ ($J^\pi = 2^+$) bosons and octupole $f$ ($J^\pi = 3^-$) bosons [11]. The following $sdf$-IBM Hamiltonian is used:

$$\hat{H} = \epsilon_d \hat{n}_d + \epsilon_f \hat{n}_f + \kappa_2 \hat{Q}\cdot\hat{Q} + \alpha \hat{L}_d \cdot \hat{L}_d + \kappa_3 : \hat{V}_3^\dagger \cdot \hat{V}_3 :$$

where $\hat{n}_d = d^\dagger \cdot \tilde{d}$ and $\hat{n}_f = f^\dagger \cdot \tilde{f}$ denote the $d$ and $f$ boson number operators, respectively. The third term is the quadrupole-quadrupole interaction with $\hat{Q} = s^\dagger \tilde{d} + d^\dagger s + \chi_d [d^\dagger \times \tilde{d}]^{(2)} + \chi_f [f^\dagger \times \tilde{f}]^{(2)}$, while $\hat{L}_d = \sqrt{10}[d^\dagger \times \tilde{d}]^{(1)}$. The last term denotes octupole-octupole interaction expressed in normal-ordered form with $\hat{V}_3^\dagger = s^\dagger \tilde{f} + \chi_3 [d^\dagger \times \tilde{f}]^{(3)}$.

For each nucleus the Hamiltonian parameters $\epsilon_d$, $\epsilon_f$, $\kappa_2$, $\kappa_3$, $\chi_d$, $\chi_f$ and $\chi_3$ are determined so that the microscopic self-consistent mean-field energy surface is mapped onto the equivalent IBM energy surface, that is, expectation value of the IBM Hamiltonian $\langle\phi|\hat{H}|\phi\rangle$ in the boson condensate state $|\phi\rangle$ [12] (see [4] for details). Here $|\phi\rangle = \frac{1}{\sqrt{N_B!}}(\lambda^\dagger)^{N_B}|-\rangle$, with $\lambda^\dagger = s^\dagger + \beta_2 d_0^\dagger + \beta_3 f_0^\dagger$. $N_B$ and $|-\rangle$ denote the number of bosons, that is, half the number of valence nucleons [13], and the boson vacuum (a core with doubly-closed shells), respectively. By equating at each point on the $(\beta_2, \beta_3)$ plane the expectation value of the $sdf$ IBM Hamiltonian to the microscopic energy surface in the neighborhood of the minimum, the Hamiltonian parameters can be determined without invoking any further adjustment to data. The coefficient $\alpha$ is determined by taking into account the rotational response in the cranking calculation [14]. Once all the parameters are obtained, the mapped Hamiltonian of diagonalized numerically, using the code OCTUPOLE [15], to generate energy spectra and transition rates.

## 3 Results of spectroscopic calculation

A signature of stable octupole deformation is a low-lying negative-parity band $J^\pi = 1^-, 3^-, 5^-, \ldots$ located close in energy to the positive-parity ground-state band $J^\pi = 0^+, 2^+, 4^+, \ldots$, thus forming an alternating-parity band. Such alternating bands are typically observed for states with spin $J \geq 5$ [1]. In the case of octupole vibrations the negative-parity band is found at higher energy, and the two sequences of positive- and negative-parity states form separate collective bands. Therefore, a systematic increase with nucleon number of the energy of the negative-parity band relative to the positive-parity ground-state band indicates a transition from stable octupole deformation to octupole vibrations [1].

In Fig. 2 we display the systematics of the calculated excitation energies of the positive-parity ground-state

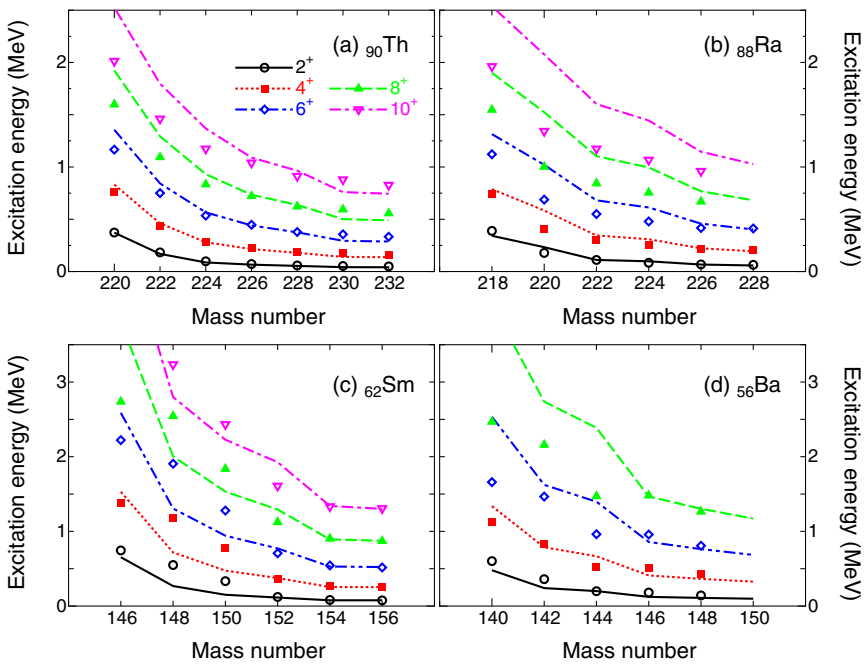


**Figure 2.** (Color online) Excitation energies of low-lying yrast positive-parity states of $^{220-232}$Th, $^{218-228}$Ra, $^{146-156}$Sm and $^{140-150}$Ba, as functions of the mass number. In each panel lines and symbols denote the theoretical and experimental [16] values, respectively.

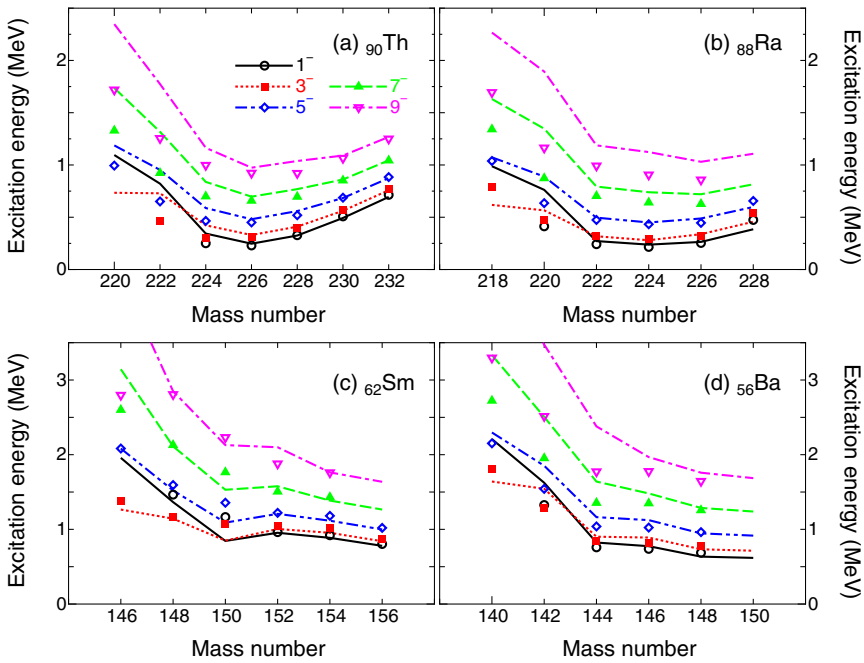


**Figure 3.** (Color online) Same as in the caption to Fig. 2 but for the negative-parity states.

band, and in Fig. 3 the lowest negative-parity sequences in $^{220-232}$Th, $^{218-228}$Ra, $^{146-156}$Sm and $^{140-150}$Ba nuclei, in comparison with available data [16]. Firstly we note that, even without any additional adjustment of the parameters to data, the IBM quantitatively reproduces the mass dependence of the excitation energies of levels that belong to the lowest bands of positive and negative parity.

The excitation energies of positive-parity states systematically decrease with mass number, reflecting the increase of quadrupole collectivity. For instance, $^{220,222}$Th exhibit a quadrupole vibrational structure, whereas pronounced ground-state rotational bands with $R_{4/2} = E(4_1^+)/E(2_1^+) \approx 3.33$ are found in $^{226-232}$Th. A similar systematics is found in the other isotopic chains (Figs. 2(b-

d)). However, the theoretical predictions for the positive-parity states with higher spin overestimate the experimental values. The discrepancies are larger for the Ra and Ba isotopes because the boson model space is more restricted in comparison to the neighboring Th and Sm isotopes.

For the states of the negative-parity band in Th isotopes the excitation energies display a parabolic structure centered between $^{224}$Th and $^{226}$Th (Fig. 3(a)). The approximate parabola of $1_1^-$ states has a minimum at $^{226}$Th, in which the octupole minimum is most pronounced. Starting from $^{226}$Th the energies of negative-parity states systematically increase and the band becomes more compressed. A rotational-like collective band based on the octupole vibrational state, i.e., the $1_1^-$ band-head, develops.

For the Ra isotopes shown in Fig. 3(b) a similar trend of negative-parity yrast states is predicted particularly for states with spin $J^\pi = 1^-, 3^-$ and $5^-$. One notices that the parabolic dependence is not as pronounced as in Th. The model predicts that the excitation energy of the $1_1^-$ state is lowest in $^{224}$Ra. This result is consistent with the evolution of the experimental low-spin negative-parity states with neutron number [16], and also with the recent experimental study of stable octupole deformation in $^{224}$Ra [2]. On the other hand, in both the positive and negative parity bands some high-spin states, particularly for the lighter isotopes, are predicted at much higher energies compared to the data [16]. One of the reasons is certainly the restricted valence space from which boson states are built.

For the Sm (Fig. 3(c)) and Ba (Fig. 3(d)) isotopes, the mass dependence of negative-parity yrast states is more monotonous. For Sm the calculated excitation energies of both positive- and negative-parity states show a very weak variation with mass number starting from $^{152}$Sm or $^{154}$Sm. The yrast states of Ba isotopes display no significant structural change starting from $^{144}$Ba or $^{146}$Ba, namely, the excitation energies of both positive- and negative-parity yrast states look almost constant with mass (neutron) number. Note, however, that the calculated energy levels for Ba isotopes exhibit a more abrupt change from $^{144}$Ba to $^{146}$Ba, especially for higher-spin states.

Another indication of the phase transition between octupole deformation and octupole vibrations for $\beta_3$-soft potentials is provided by the odd-even staggering in the energy ratio $E(J)/E(2_1^+)$. Figure 4 displays the ratios $E(J)/E(2_1^+)$ for both positive- and negative-parity yrast states as functions of the angular momentum $J$, taking Th isotopes as an example. Below $^{226}$Th the odd-even staggering is negligible, indicating that positive and negative parity states are lying close to each other in energy. The staggering only becomes more pronounced starting from $^{228}$Th, and this means that negative-parity states form a separate rotational band built on the octupole vibration. The predicted staggering of yrast states is in very good agreement with data [16].

To illustrate in more detail the level of quantitative agreement between the present calculation and data, in Fig. 5 we display the relevant energy spectrum in the octupole-soft nucleus $^{230}$Th, including the in-band $B$(E2) values and the $B(\mathrm{E3}; 3_1^- \to 0_1^+)$ (both in Weisskopf units),

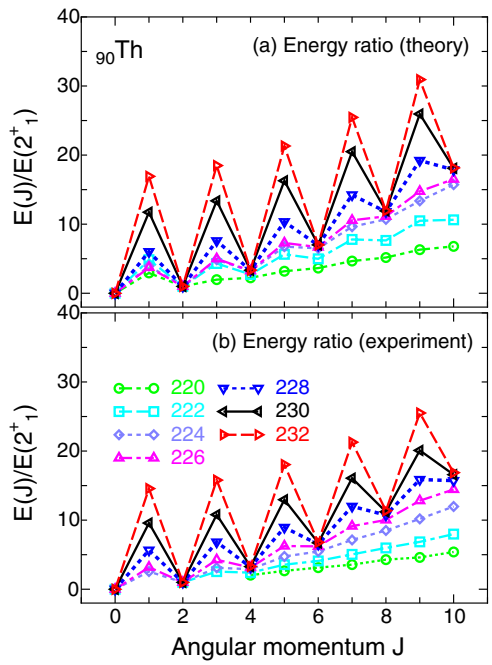


**Figure 4.** (Color online) Theoretical (a) and experimental [16] (b) energy ratios $E(J)/E(2_1^+)$ of the yrast states of $^{220-232}$Th, including both positive ($J$ even) and negative ($J$ odd) parity, as functions of the angular momentum $J$.

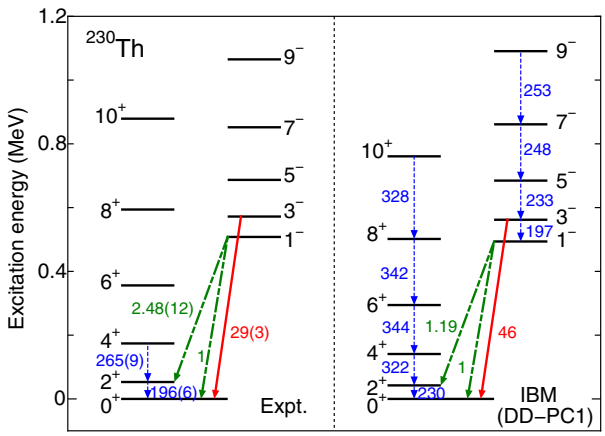


**Figure 5.** Experimental and calculated yrast states in $^{230}$Th. The in-band $B$(E2) (dotted) and the $B$(E3) (solid) values (both in Weisskopf units), and the branching ratio $B(\mathrm{E1}; 1_1^- \to 2_1^+)/B(\mathrm{E1}; 1_1^- \to 0_1^+)$ (dashed-dotted) are also shown.

and the branching ratio $B(\mathrm{E1}; 1_1^- \to 2_1^+)/B(\mathrm{E1}; 1_1^- \to 0_1^+)$. The E1, E2 and E3 operators read $\hat{T}^{(\mathrm{E1})} = e_1(d^\dagger \times \tilde{f} + f^\dagger \times \tilde{d})^{(1)}$, $\hat{T}^{(\mathrm{E2})} = e_2\hat{Q}$ and $\hat{T}^{(\mathrm{E3})} = e_3(\hat{V}_3^\dagger + \hat{V}_3)$, respectively, with $e_2$ and $e_3$ being the effective charges. One notices a very good agreement with experiment, not only for excitation energies but also for transition probabilities.

Finally, we compare the results of the present microscopic calculation with very recent data for the octupole deformed nucleus $^{224}$Ra, obtained in the Coulomb excita-

**Table 1.** Comparison between experimental [2] and theoretical $B(\mathrm{E}\lambda)$ values in $^{224}$Ra.

| | Expt. (W.u.) | Theor. (W.u.) |
|---|---|---|
| $B(\mathrm{E2}; 2_1^+ \to 0_1^+)$ | 98±3 | 109 |
| $B(\mathrm{E2}; 3_1^- \to 1_1^-)$ | 93±9 | 71 |
| $B(\mathrm{E2}; 4_1^+ \to 2_1^+)$ | 137±5 | 152 |
| $B(\mathrm{E2}; 5_1^- \to 3_1^-)$ | 190±60 | 97 |
| $B(\mathrm{E2}; 6_1^+ \to 4_1^+)$ | 156±12 | 159 |
| $B(\mathrm{E2}; 8_1^+ \to 6_1^+)$ | 180±60 | 153 |
| $B(\mathrm{E2}; 2_2^+ \to 0_1^+)$ | 1.3±0.5 | 0 |
| $B(\mathrm{E3}; 3_1^- \to 0_1^+)$ | 42±3 | 42 |
| $B(\mathrm{E3}; 1_1^- \to 2_1^+)$ | 210±40 | 85 |
| $B(\mathrm{E3}; 3_1^- \to 2_1^+)$ | <600 | 46 |
| $B(\mathrm{E3}; 5_1^- \to 2_1^+)$ | 61±17 | 61 |
| $B(\mathrm{E1}; 1_1^- \to 0_1^+)$ | $< 5 \times 10^{-5}$ | $2.0\times10^{-3}$ |
| $B(\mathrm{E1}; 1_1^- \to 2_1^+)$ | $< 1.3 \times 10^{-4}$ | $1.1\times10^{-3}$ |
| $B(\mathrm{E1}; 3_1^- \to 2_1^+)$ | $3.9^{+1.7}_{-1.4} \times 10^{-5}$ | $3.7\times10^{-3}$ |
| $B(\mathrm{E1}; 5_1^- \to 4_1^+)$ | $4^{+3}_{-2} \times 10^{-5}$ | $5.0\times10^{-3}$ |
| $B(\mathrm{E1}; 7_1^- \to 6_1^+)$ | $< 3 \times 10^{-4}$ | $5.8\times10^{-3}$ |

tion experiment of Ref. [2]. Table 1 lists all the experimental $B(\mathrm{E}\lambda)$ values included in Ref. [2], in comparison with our model results. For the E2 transition rates a very good agreement is obtained between the experimental and the calculated values, possibly with the exception of the $5^- \to 3^-$ transition which is underestimated in the calculation. We also note the nice agreement of the $B(\mathrm{E3}; J \to J-3)$ values, but the calculated $B(\mathrm{E3}; 1^- \to 2^+)$ is considerably smaller than the experimental value. On the other hand, the theoretical $B(\mathrm{E1})$ values are systematically too large, typically by $10^1 - 10^2$, when compared with data. There are several possible reasons for this discrepancy: (i) the constant value of the E1 effective charge, (ii) the restricted form of the adopted E1 operator, and (iii) the insufficient $sdf$ model space that could be extended by the inclusion of other types of bosons.

## 4 Summary and concluding remarks

In the present study we have performed a microscopic analysis of octupole shape transitions in several isotopic chains characteristic for octupole deformation and collectivity. As a microscopic input we have used the axial quadrupole-octupole deformation energy surfaces calculated employing the RHB model based on the DD-PC1 functional, which has not been specifically adjusted to octupole deformed nuclei. By mapping the deformation-constrained microscopic energy surfaces onto the equivalent $sdf$ IBM Hamiltonian, the Hamiltonian parameters have been determined without any specific adjustment to experimental spectra. The mapped $sdf$ IBM Hamiltonian has been used to calculate low-energy spectra and transition rates for both positive- and negative-parity states of the four sequences of isotopes. The systematics of the calculated results show a consistent picture of evolution of octupole correlations in the two regions of medium-heavy and heavy nuclei. For most nuclei considered in the present analysis the IBM model based on microscopic deformation energy surfaces produces results in a reasonable agreement with available experimental spectroscopic properties, apart from a major discrepancy found in the description of the E1 transitions, which is the topic of a future study.

## Acknowledgment

The author acknowledges D. Vretenar, T. Nikšić, and B.-N. Lu for collaboration on this subject, T. Otsuka and N. Shimizu for a number of valuable discussions, and the support by the Marie Curie Intra-European Fellowship within the Seventh Framework Program of the European Commission under Grant No. PIEF-GA-2012-327398.

## References

[1] P. A. Butler, and W. Nazarewicz, Rev. Mod. Phys. **68**, 349 (1996)

[2] L. P. Gaffney et al., Nature (London) **497**, 199 (2013)

[3] M. Bender, P.-H. Heenen, and P.-G. Reinhard, Rev. Mod. Phys. **75**, 121 (2003)

[4] K. Nomura, N. Shimizu, and T. Otsuka, Phys. Rev. Lett. **101**, 142501 (2008)

[5] F. Iachello and A. Arima, *The interacting boson model* (Cambridge University Press, Cambridge, UK, 1987)

[6] K. Nomura, D. Vretenar, and B.-N. Lu, Phys. Rev. C **88**, 021303(R) (2013)

[7] K. Nomura, D. Vretenar, T. Nikšić, and B.-N. Lu, Phys. Rev. C **89**, 024312 (2014)

[8] T. Nikšić, D. Vretenar, and P. Ring, Prog. Part. Nucl. Phys. **66**, 519 (2011)

[9] B.-N. Lu et al., Phys. Rev. C **89**, 014323 (2014)

[10] T. Nikšić, D. Vretenar, and P. Ring, Phys. Rev. C **78**, 034318 (2008)

[11] J. Engel and F. Iachello, Nucl. Phys. A **472**, 61 (1987).

[12] J. N. Ginocchio and M. W. Kirson, Nucl. Phys. A **350**, 31 (1980)

[13] T. Otsuka, A. Arima, and F. Iachello, Nucl. Phys. A **309**, 1 (1978)

[14] K. Nomura, T. Otsuka, N. Shimizu, and L. Guo, Phys. Rev. C **83**, 041302(R) (2011)

[15] D. Kusnezov, computer program OCTUPOLE (unpublished)

[16] NNDC, http://www.nndc.bnl.gov